



# Influence of ferrite stabilizing elements and Co on structure and magnetic properties of carbon-encapsulated iron nanoparticles synthesized in thermal plasma jet



Z. Karoly<sup>a</sup>, J. Szepvolgyi<sup>a,b</sup>, W. Kaszuwara<sup>c</sup>, O. Łabędź<sup>d</sup>, M. Bystrzejewski<sup>d,\*</sup>

<sup>a</sup> Research Centre for Natural Sciences, Hungarian Academy of Sciences, Magyar Tudósok krt. 2. 1117 Budapest, Hungary

<sup>b</sup> Research Institute of Chemical and Process Engineering, University of Pannonia, Egyetem u. 2. 8200 Veszprém, Hungary

<sup>c</sup> Warsaw University of Technology, Faculty of Materials Science and Engineering, Wołoska 141 str., 02-507 Warsaw, Poland

<sup>d</sup> University of Warsaw, Dept of Chemistry, Pasteur 1 str., 02-093 Warsaw, Poland

## ARTICLE INFO

### Article history:

Received 5 July 2014

Received in revised form 4 September 2014

Accepted 5 September 2014

Available online 16 September 2014

### Keywords:

Magnetic materials  
Magnetic properties  
Phase composition  
Austenite  
Annealing

## ABSTRACT

The encapsulation of Fe nanoparticles in protective carbon coatings always leads to formation of undesired paramagnetic austenite phase. Various ferrite stabilizing elements were included in the synthesis process to verify whether their inclusion may minimize the austenite content in carbon-encapsulated iron nanoparticles synthesized in thermal plasma jet. Eight ferrite stabilizing elements (Si, Al, Mo, Ti, Zr, Cr, W and V) and one austenite promoting additive (Co) were tested. Their influence on the synthesis yield, phase composition, morphology and magnetic properties of carbon-encapsulated iron nanoparticles was studied. It was found that the addition of ferrite stabilizers strongly influences the diameter distribution, graphitization degree, phase composition and magnetic properties. Contrary to the thermodynamic predictions the inclusion of ferrite stabilizing elements caused a substantial worsening of magnetic performance in carbon-encapsulated iron nanoparticles. It has been also shown that the subsequent heat treatment of carbon-encapsulated iron nanoparticles significantly improves their magnetic properties.

© 2014 Elsevier B.V. All rights reserved.

## 1. Introduction

Carbon-encapsulated magnetic nanoparticles, frequently named as “carbon encapsulates”, are a core–shell type nanomaterial with a broad perspective of applications. Generally, the shell in these nanostructures is of great importance, because it effectively protects the core material from unwanted and uncontrollable processes, e.g. oxidation, corrosion and agglomeration [1]. Carbon encapsulates are considered as a unique platform which delivers a very original solution to preserve the inherent physical and chemical properties of bare metal nanoparticles. The carbon coating in carbon encapsulates is the best coating agent among other encapsulating materials (gold, polymers, boron nitride) because it is light, impermeable and has high stability in contact with various aggressive chemical reagents (non-oxidative mineral and organic acids, bases, greases, oils) [2]. Moreover, the carbon coating possesses high thermal stability because it does not undergo gasification under oxygen atmosphere at temperature below 400–450 °C [3].

Carbon-encapsulated magnetic nanoparticles can be fabricated by a variety of synthesis routes. These approaches can be divided into (i) low temperature and (ii) high temperature routes. The first group primarily includes pyrolysis based processes and chemical vapor deposition [4–7]. The low temperature approaches do not require large energy input, however on the other hand have limited selectivity [7]. The high temperature routes (e.g. carbon arc discharge, thermal plasma, flame spray synthesis) consume more energy, however, are capable to fabricate carbon encapsulates in a continuous manner and with high selectivity [8–10,6]. Iron is the most frequent encapsulated element in carbon. This is because of the best magnetic performance of Fe over other transition metals. Unfortunately, the encapsulation of Fe always leads to broad phase composition. The products contain *bcc* Fe, Fe<sub>3</sub>C and *fcc* Fe–C (austenite) nanoparticles encapsulated in carbon. The presence of austenite is highly undesirable because this phase is paramagnetic (at room temperature) and diminishes the overall magnetic moment. The data published in previous papers show that the relative amount of austenite in carbon-encapsulated iron nanoparticles (CEINs) can reach even 30% [11,12]. The goal of this work is to verify whether the inclusion of ferrite stabilizing elements (FSE) in

\* Corresponding author. Tel.: +48 22 822 02 11.

E-mail address: [mibys@chem.uw.edu.pl](mailto:mibys@chem.uw.edu.pl) (M. Bystrzejewski).

the synthesis process of carbon-encapsulated iron nanoparticles may minimize the formation of unwanted austenite phase. The thermodynamic predictions of the Fe–FSE system evidence that the presence of all studied elements hampers the formation of austenite and stabilize the ferrite phase. The phase diagrams of these Fe–FSE systems are shown in [Supplementary Data](#). This work partially corresponds to the previous paper in which the influence of Al on magnetic properties of carbon-encapsulated iron nanoparticles synthesized via carbon arc discharge was studied [13].

## 2. Experimental

The synthesis of carbon-encapsulated iron nanoparticles was carried out using a flow-through radio frequency thermal plasma reactor. The reactor comprises of two sections, i.e. the plasma torch and the water-cooled chamber, in which the products undergo condensation. The experimental system was described in details elsewhere [14]. All tests were carried out under atmospheric pressure. The RF power (22–23 kW) was supplied by a generator operating at 2–3 MHz. Argon was used as a plasma gas (15 slpm), while the sheath gas was Ar (40 slpm) mixed with He (20 slpm). The starting reactants (Fe powder, an additive and ethanol) were axially introduced via a water-cooled probe located at the center of the plasma torch. Ethanol (purity at least 98%) was fed by a pneumatic feeder with a flow rate of  $12.5 \pm 1.5$  ml/min. The Fe powder with the mean grain size of 6–9  $\mu\text{m}$  (as declared by the manufacturer) was used. Nine various additives (Si, Al, Mo, Ti, Zr, Cr, W, V and Co) were in a form of fine powders (the mean grain size between 10  $\mu\text{m}$  and 50  $\mu\text{m}$ ). The metal powders (pure Fe or Fe-additive mixture (90–10 wt.%) were delivered to the torch by argon (5 slpm) with a feed rate of 1.6–5.8 g/min. The feed rate for each delivered mixture and the corresponding flow rate of the collected product are given in [Table S1](#) (see [Supplementary Data](#)).

The as-synthesized (raw) products were collected from the reactor walls only. In each test some amount of the solid products were also present in the bottom of the reactor. These products consisted primarily of the non-processed starting metal particles, and therefore they were not collected. The raw products were subjected to purification in order to irreversibly remove the non-encapsulated metallic particles and these particles, which were encapsulated in permeable (defected) carbon coatings. The purification procedure included 24 h of boiling in 3 M HCl with subsequent washing with excess water and ethanol. The mass of the product recovered after purification was monitored. The chemical composition of the raw and purified products was evaluated by thermogravimetry under oxygen atmosphere (the full procedure and the corresponding curves are shown in [Supplementary Data](#)). The morphology of the raw and purified products was studied by transmission electron microscopy (TEM, Zeiss Libra 120 operated at 120 kV). The phase composition studies were conducted on a Bruker D8 diffractometer using a Cu K $\alpha$  radiation in a  $2\theta$  range between 10 and 70 with a step of 0.02 deg. Raman spectra were acquired using a dispersive spectrometer (Jobin Ivon T-64000) equipped a 514.5 nm excitation laser. Magnetic measurements were carried out at 25 °C using a vibrating magnetometer (Lake Shore 668). The measured magnetization was referred to the total mass of the studied sample.

## 3. Results and discussion

### 3.1. Process efficiency

[Fig. 1a](#) shows the product formation rate of carbon-encapsulated iron nanoparticles. The product formation rate is defined as the ratio of the flow rate of the collected product from the reactor walls and the total feed rate of the starting reagents (i.e. ethanol, Fe and the additive). Generally, the product formation rate for most of the used additives is between 5% and 8%. A substantially higher value is observed for the test conducted with the inclusion of W (11%) and Zr (18%). The higher values of the product formation rate plausibly result from the presence of corresponding carbides, which may interfere the product formation rate (i.e. WC and ZrC, see [Section 3.3](#) for more details). [Fig. 1b](#) shows the purification yield for CEINs synthesized with the addition of various ferrite stabilizing additives. The purification yield is defined as the ratio of the starting and the recovered mass of the sample which was subjected to purification. In other words, the purification yield visualizes how much of the raw product is irreversibly dissolved during acid treatment. The purification yield varies in a relatively broad range, i.e. between 23% and 52%. For the correct interpretation of these results one has to

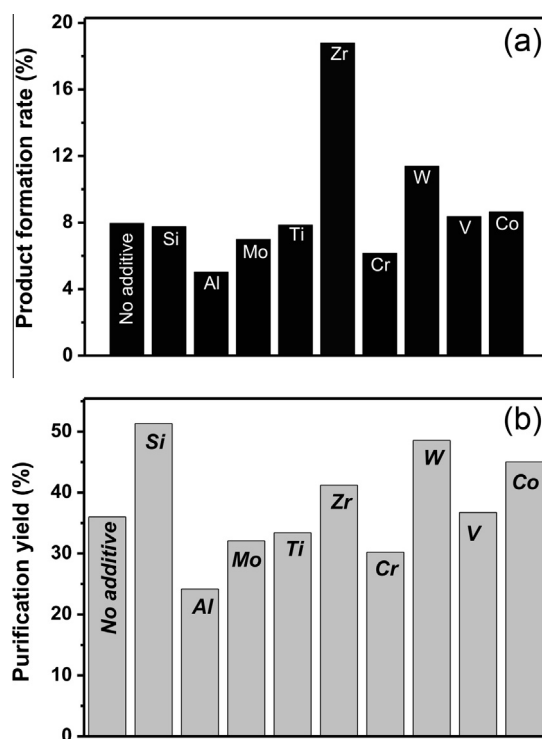


**Fig. 1.** Product formation rate (a) and purification yield (b) of carbon-encapsulated iron nanoparticles synthesized with addition of various ferrite stabilizing elements.

refer to chemical stability of the additives (and the corresponding carbides) in boiled 3 M HCl. Iron, cobalt, aluminum, titanium and chromium are the metals that are readily soluble in hydrochloric acid. The other studied additives (W, Zr, V, Mo and Si) are resistant to HCl. Among the carbides, only  $\text{Al}_4\text{C}_3$  and  $\text{Co}_2\text{C}$  are the compounds that are easily leached by hydrochloric acid. The pattern in [Fig. 2](#) shows that the products synthesized with the inclusion of Si, Zr, W and Co plausibly contain, in addition to CEINs, carbides or pure metal crystallites, which can appear in the encapsulated and non-encapsulated form.

The data from [Fig. 1a](#) and [b](#) along with the operational details from [Table S1](#) can be used to estimate the overall process efficiency. The overall process efficiency (TPE) is a number, which determines the mass of the purified products, which is available in a unit of time (e.g. g/h). This parameter can be calculated in the following way:  $TPE \text{ (g/h)} = PFR \cdot PY \cdot FRS \text{ (g/h)}$ , where TPE is the overall process efficiency, PFR is the product formation rate (dimensionless), PY is the purification yield (dimensionless) and FRS is the flow rate of the starting reagents (i.e. ethanol, iron and the additive). The TPE values are shown in [Fig. S1](#). The pattern in [Fig. S1](#) is generally similar to the diagrams presented in [Figs. 1 and 2](#). The process efficiency varies between ca. 9 g/h for (Al) and ca. 62 g/h (Zr). The data show that the inclusion of W and Zr results in a (at least) 1.5-fold increase of the process efficiency.

### 3.2. Morphology

The representative TEM images of the products are shown in [Fig. 2](#). Irrespective of the applied additive the samples contain nanosized particles. The nanoparticles are covered by a thin carbon coating (a few nm in thickness). This observation directly proves that the encapsulation process was successful. In the case of the sample obtained from pure Fe (without any addition) most of the nanoparticles have the diameter in the range between 10 nm and 70 nm ([Fig. 2a](#)). The inclusion of ferrite stabilizing elements

Download English Version:

<https://daneshyari.com/en/article/8000680>

Download Persian Version:

<https://daneshyari.com/article/8000680>

[Daneshyari.com](https://daneshyari.com)